

# Search for $\Theta^+(1540)$ emission in hadron–nucleus collisions at 400–700 GeV

A. E. Asratyan and V. A. Matveev

*Institute of Theoretical and Experimental Physics, Moscow, 117218 Russia*

Email: ashot.asratyan@gmail.com, matveev@itep.ru

September 3, 2016

## Abstract

The data on hadron–nucleus collisions at 400–700 GeV, collected by the SELEX experiment at Fermilab, are analyzed for formation of the exotic pentaquark baryon  $\Theta^+(1540)$ . A narrow enhancement near 1539 MeV is observed in the mass spectrum of the  $pK_S^0$  system emitted at small  $x_F$  from hadron collisions with copper nuclei. The statistical significance of the peak is near 9 standard deviations. Fitted width of the observed  $pK_S^0$  resonance is consistent with being entirely due to experimental resolution, and its intrinsic width is restricted to  $\Gamma < 3$  MeV at 90% CL. The data favor positive rather than negative strangeness for the  $pK_S^0$  resonance observed in  $h\text{Cu}$  collisions. At the same time, the  $pK_S^0$  mass spectrum for collisions in carbon is featureless. The yield of  $\Theta^+$  baryons per  $h\text{C}$  collision is restricted to be  $< 24\%$  of the yield per  $h\text{Cu}$  collision.

Possible existence of multiquark hadrons, and pentaquark baryons in particular, has been discussed ever since the quark model was proposed [1]. Fairly definite predictions for the antidecuplet of pentaquark baryons with spin–parity  $1/2^+$  have been formulated by Diakonov, Petrov, and Polyakov in the framework of the chiral quark–soliton model [2]. Their crucial prediction has been that the explicitly exotic baryon with  $S = +1$  and  $I = 0$ , the  $\Theta^+(uudd\bar{s})$  that should decay to  $nK^+$  and  $pK^0$ , is relatively light and narrow:  $m \approx 1530$  MeV and  $\Gamma < 15$  MeV. More recent theoretical analyses suggest that the  $\Theta^+$  intrinsic width may be as small as  $\sim 1$  MeV or even less [3]. Narrow peaks near 1540 MeV in the  $nK^+$  and  $pK^0$  mass spectra were initially detected in low-energy photoproduction by LEPS [4] and in the charge-exchange reaction  $K^+n \rightarrow pK^0$  by DIANA [5]. Yet another early observation in the  $pK^0$  channel, that endured the time test, relied on combined bubble-chamber data on  $\nu N$  collisions [6]. Subsequently, both LEPS and DIANA were able to confirm their initial observations [7, 8, 9, 10, 11]. Using the unique properties of the charge-exchange reaction that forms  $\Theta^+$  baryons in the  $s$ -channel, DIANA reported a direct measurement of the  $\Theta^+$  intrinsic width:  $\Gamma = 0.34 \pm 0.10$  MeV assuming  $J = 1/2$  [10].

Other searches for the  $\Theta^+$  baryon in different reactions and experimental conditions yielded positive evidence as well as null results casting doubt on its existence, see the review papers [12, 13, 14]. One of the heftiest null results was reported by CLAS using a large sample of  $\gamma p$  collisions [15]. However, the same sample was later reanalyzed in terms of  $\phi p$  and  $\Theta^+ \bar{K}^0$  interference in the  $pK_S^0 K_L^0$  final state, and a statistically significant peak near 1539 MeV was found in the  $K_S^0$  missing mass [16]. Of the multitude of null results, only a few that are formulated in terms of the  $\Theta^+$  intrinsic width  $\Gamma$  should be treated as physically meaningful. The best upper limit to date,  $\Gamma < 0.36$  MeV assuming  $J^P = 1/2^+$ , was obtained in [17] by analyzing the  $K^-$  missing mass in the  $\pi^- p \rightarrow K^- X$  reaction. This restriction is narrowly consistent with the DIANA measurement. The bulk of null results can be probably explained by the extreme smallness of the  $\Theta^+$  width that implies the smallness of production cross-sections [18].

The properties of the pentaquark baryon  $\Theta^+(1540)$  can be best probed in low-energy exclusive processes such as the charge-exchange reaction  $K^+n \rightarrow pK^0$ . In high-energy collisions, Azimov *et al.* argue that the  $\Theta^+$  baryon should be primarily formed from multiquark configurations of the target residue [19], and therefore emitted with small  $x_F$ . In this report, we investigate the  $pK_S^0$  mass spectrum in SELEX, paying special attention to the kinematic region of target fragmentation.

The SELEX experiment operated in the Fermilab hyperon beam, and was primarily

designed for studying hadroproduction of charmed baryons and mesons in the forward region. The negative beam at  $\langle p_{\text{beam}} \rangle = 615$  GeV was composed of about 50%  $\Sigma^-$  and 50%  $\pi^-$ . The positive beam at  $\langle p_{\text{beam}} \rangle = 540$  GeV was 92% protons. The beam spread was  $\Delta p/p \simeq 8\%$  HWHM. A beam Transition Radiation Detector identified each beam particle as meson or baryon with zero overlap. The beam interacted in a set of five target foils ( 2 Cu and 3 C) spaced by 1.5 cm. Target thickness was 1.06% and 0.76%  $\lambda_{\text{int}}$  for the two copper targets, and 0.82%  $\lambda_{\text{int}}$  for each of the three carbon targets. As part of the triggering system, one scintillation counter was placed upstream and two—downstream of the target assembly. The three-stage magnetic spectrometer is shown elsewhere [20]. The most important features are the high-precision, highly redundant vertex detector that provides an average proper-time resolution of 20 fs for the charm decays, a 10-m-long Ring-Imaging Cherenkov (RICH) detector that separates  $\pi$  from  $K$  up to 165 GeV/c [21], and a high-resolution tracking system that has momentum resolution of  $\sigma_p/p < 1\%$  for a 150-GeV proton. The triggering scheme was optimized for selecting charm candidate events. A scintillator trigger demanded an inelastic collision with at least four charged tracks in the interaction scintillators and at least two hits in the positive-particle hodoscope after the second analyzing magnet. Event selection in the online filter required full track reconstruction for measured fast tracks ( $p > 15$  GeV). These tracks were extrapolated back into the vertex silicon planes and linked to silicon hits. The beam track was measured in upstream silicon detectors. A full three-dimensional vertex fit was then performed. An event was logged on tape if any of the fast tracks in the event were *inconsistent* with having come from a single primary vertex. This filter passed 1/8 of all interaction triggers. The experiment recorded data from  $15.2 \times 10^9$  inelastic interactions and logged  $1 \times 10^9$  events on tape using both positive and negative beams. The sample was 67%  $\Sigma^-$ -induced, 14%  $\pi^-$ -induced, and 18% proton-induced.

We analyze the complete SELEX dataset reconstructed using standard routines plus some extra algorithms that allow to detect more secondary vertices [22]. In particular, additional Vee particles that decayed inside the vertex detector are reconstructed by extrapolating spectrometer tracks back to the vertex detector and matching them with hits in Silicon planes. Prior to analysis selections, we have some 8.4 million reconstructed  $K_S^0 \rightarrow \pi^+\pi^-$  decays above large combinatorial background, see Fig. 1a. The reconstruction of pre-selected  $\pi^+\pi^-$  decays of  $K_S^0$  mesons with  $p < 20$  GeV is separately illustrated in Fig. 1b. As soon as we are primarily interested in  $pK_S^0$  pairs emitted in the kinematic region of target fragmentation, special attention must be paid to selecting relatively soft  $K_S^0 \rightarrow \pi^+\pi^-$  and proton candidates. The selections used in this analysis are described below.

The primary vertex of the collision is found using the standard algorithm. The beam track should be accurately reconstructed ( $\chi^2 < 9$ ), and is always retained when iteratively fitting the primary vertex. For the latter, we require  $\chi^2 < 6$ . The fitted primary vertex should lie either inside target material or within  $500 \mu\text{m}$  of the target. (The uncertainty on the  $z$ -coordinate of the primary vertex is  $\sim 200 \mu\text{m}$  on average.) The number of secondary tracks fitted to the primary vertex is restricted to the interval  $5 < N < 20$ . This is to select deep-inelastic collisions and, on the other hand, to suppress secondary interactions and reduce the occupancy of Silicon planes.

The  $K_S^0 \rightarrow \pi^+\pi^-$  decays are selected as follows :

- $|\cos \Theta_\pi^*| < 0.75$  for the decay angle in the  $K_S^0$  frame, whereby any reflection from  $\Lambda \rightarrow p\pi^-$  is completely removed and the softest decay pions in lab are rejected ;
- $L/\sigma_L > 6$  for the  $K_S^0$  path before decay in error units, aimed at rejecting tracks emitted from the primary vertex ;
- $\text{DCA} > 20 \mu\text{m}$  for the Distance of Closest Approach between the track of either daughter pion and the beam track, further rejecting tracks from the primary vertex ;
- Either  $\chi_{\text{pvtx}}^2 < 9$  or  $\beta_{\text{miss}} < 0.5 \text{ mrad}$  for associating the Vee with the reconstructed primary vertex. Here,  $\beta_{\text{miss}}$  is the ‘‘acoplanarity’’ angle between the  $K_S^0$  decay plane and its path in lab (straight line between the primary and secondary vertices);
- $p(\pi^\pm) > 3 \text{ GeV}$  for lab momenta of both decay pions, as suggested by the momentum threshold of the spectrometer ;
- $\chi^2 < 9$  for the tracks of both daughter pions, and  $\chi^2 < 4$  for the reconstructed secondary vertex.

The combined effect of these selections on the  $K_S^0 \rightarrow \pi^+\pi^-$  signal is shown in Figs. 1c and 1d for the full  $K_S^0$  momentum interval and for  $p < 20 \text{ GeV}$ , respectively. In what follows, the  $K_S^0 \rightarrow \pi^+\pi^-$  decays are selected in the mass interval  $|m(\pi^+\pi^-) - m(K^0)| < 8 \text{ MeV}$ , which corresponds to some  $2.5\sigma$ .

Proton candidates are selected as : (a) tracks that produced Cherenkov rings, for which the proton probability is the highest according to RICH data (PID = 5); (b) tracks with momenta below the Cherenkov threshold for protons, that impinged on the RICH but have not been identified as either kaons, pions, muons, or electrons (PID = 0). The additional selections are as follows :

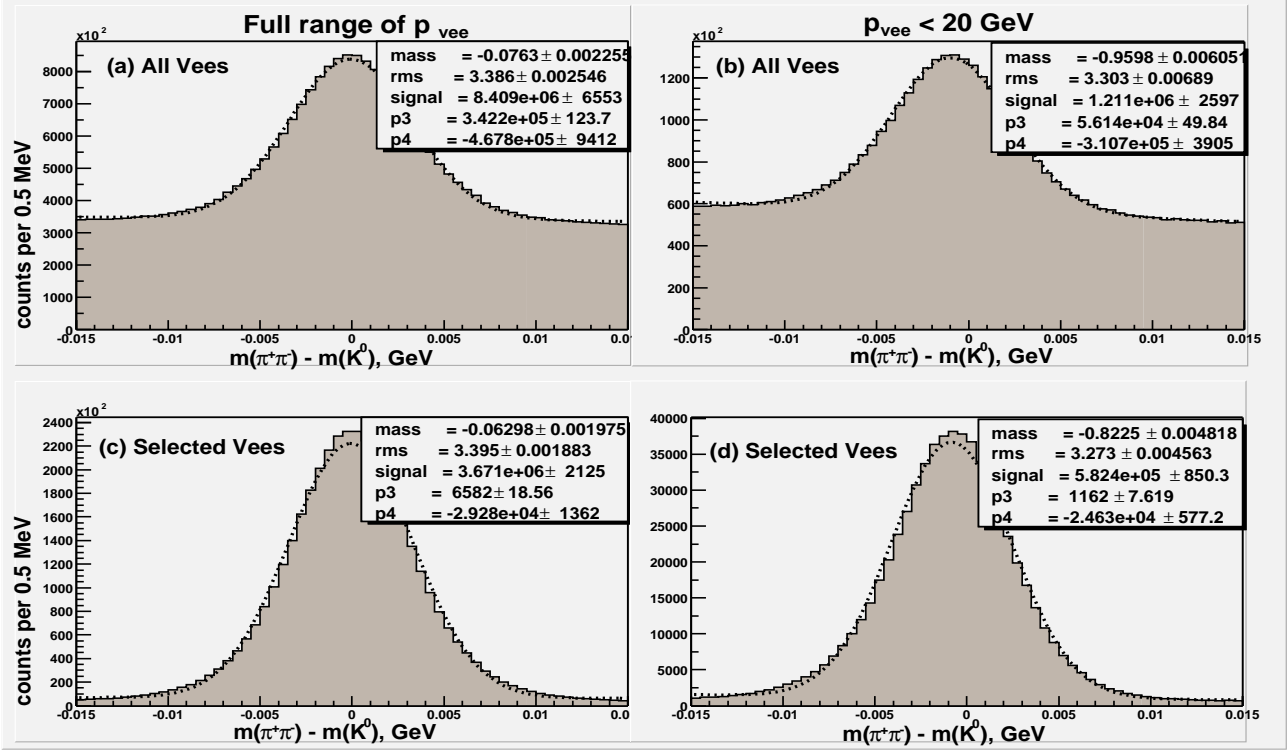


Figure 1: The effective  $\pi^+\pi^-$  mass for all detected Vees prior to analysis selections (a) and for the selected  $K_S^0 \rightarrow \pi^+\pi^-$  candidates (c). The effect of the additional selection  $p_{vee} < 20$  GeV is illustrated in the right-hand panels (b) and (d).

- The Distance of Closest Approach between the proton and beam tracks is restricted to  $DCA < 15 \mu\text{m}$  ;
- For the sub-threshold proton candidates, the RICH pion and muon probabilities must not exceed 70%, and the number of hits in the Transition Radiation Detector must not exceed 3 ;
- The proton track should be accurately reconstructed ( $\chi^2 < 6$ ) so as not to degrade the resolution on the  $pK_S^0$  effective mass.

For the instrumental smearing of  $m(\pi^+\pi^-)$  in the decay  $K_S^0 \rightarrow \pi^+\pi^-$  to cancel out, the mass of the  $pK_S^0$  system is estimated as  $m'(pK_S^0) = m(p\pi^+\pi^-) - m(\pi^+\pi^-) + m(K^0)$ . The Feynman variable is defined as  $x_F = p_L^*/p_{\text{max}}^*$ , where  $p_L^*$  is  $pK_S^0$  longitudinal momentum in the collision frame assuming a target nucleon at rest in lab, and  $p_{\text{max}}^*$  is its maximum value that corresponds to zero-mass recoil against the  $pK_S^0$  system.

The  $pK_S^0$  effective mass is plotted in Fig. 2a for all combinations of selected protons

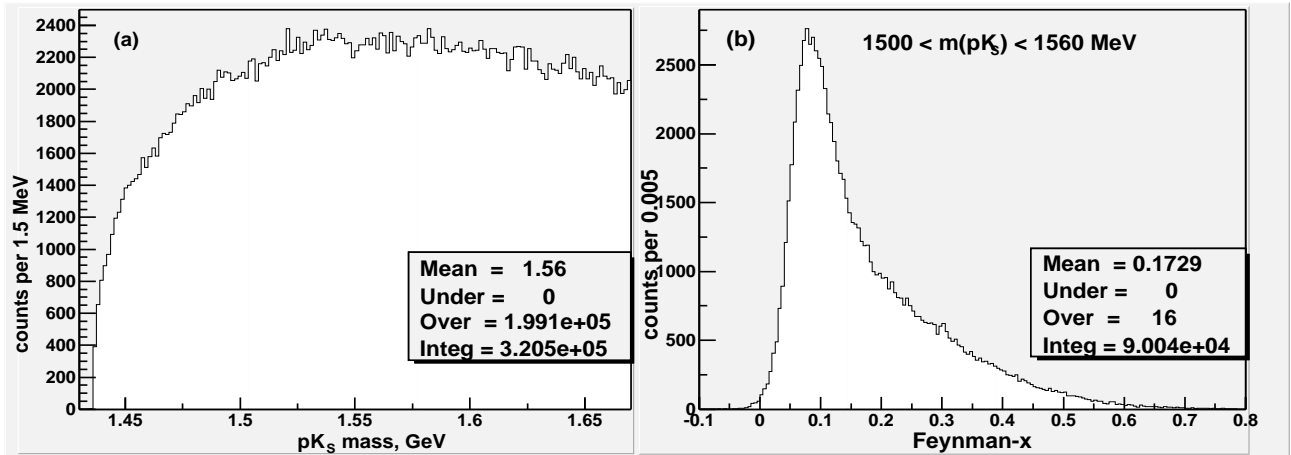


Figure 2: The  $pK_S^0$  effective mass for all combinations of selected protons and  $K_S^0$  mesons in all reconstructed events (a). Shown in (b) is the Feynman variable  $x_F$  for selected  $pK_S^0$  pairs with effective mass in the region of 1500–1560 MeV.

and  $K_S^0$  mesons in all reconstructed events. Here and in what follows, the data for the  $\Sigma^-$ ,  $\pi^-$ , and proton projectiles have been combined. The  $pK_S^0$  mass spectrum for the full range of  $x_F$  shows no significant peaks in the mass region 1520–1540 MeV. The analogous mass spectrum for the  $\bar{p}K_S^0$  system (not shown) is equally regular. That the  $x_F$  distribution shown in Fig. 2b steeply decreases towards  $x_F = 0$  is the effect of detection efficiency, *i.e.* of the losses of soft  $K_S^0$  mesons and protons. The  $x_F$  distribution for the relevant mass region  $1500 < m(pK_S^0) < 1560$  MeV is very similar to that obtained in the WA89 analysis of the  $pK_S^0$  mass spectrum [23]. Note however that the kinematic region  $x_F < 0.05$ , that we find to be the most interesting, was not investigated in [23] for some unknown reason. The effect of cutting on  $x_F$  is illustrated in Fig. 3 for either the  $pK_S^0$  and  $\bar{p}K_S^0$  mass spectra. At  $x_F$  values below some 0.05, an enhancement near 1540 MeV emerges in the  $pK_S^0$  mass spectrum for collisions reconstructed in all targets, whereas the  $\bar{p}K_S^0$  mass spectrum remains featureless. For the  $pK_S^0$  pairs with  $x_F < 0.04$ , proton and  $K_S^0$  lab momenta are plotted in Fig. 4. Virtually all contributing protons are in the sub-threshold category (PID = 0) and, moreover, uncomfortably below the charged-kaon Cherenkov threshold of some 41 GeV.

Shown in Fig. 5 is the breakdown of the  $pK_S^0$  mass spectrum for  $x_F < 0.04$  to the five targets proper plus scintillator counters (the data for the three counters have been combined because of small statistics). The puzzling result is that the peak near 1540 MeV is clearly seen in the  $pK_S^0$  mass spectra for collisions in both copper targets, but not in carbon or scintillator. The data for collisions with copper and carbon nuclei are compared in Fig. 6. The low- $x_F$  enhancement near 1540 MeV is very prominent in the  $pK_S^0$  mass spectrum for collisions in

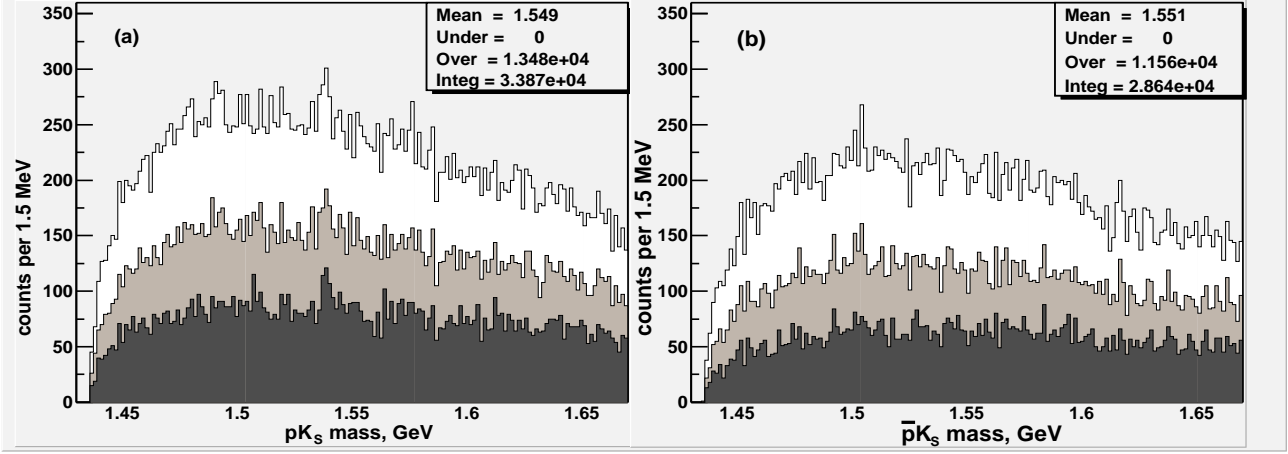


Figure 3: The  $pK_S^0$  (a) and  $\bar{p}K_S^0$  (b) mass spectra under the selections  $x_F < 0.06$ ,  $0.05$ , and  $0.04$  (the open, shaded, and dark histograms, respectively).

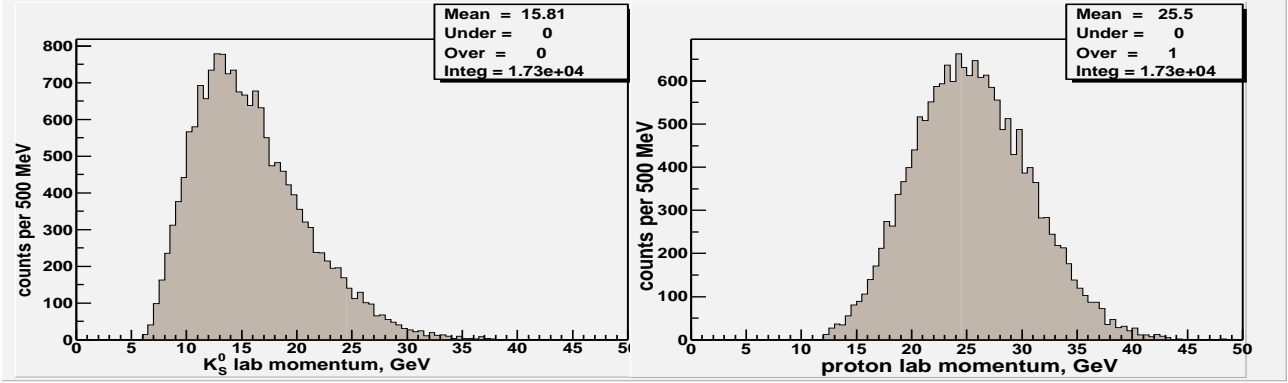


Figure 4: Lab momenta of those protons and  $K_S^0$  mesons that form  $pK_S^0$  pairs with  $x_F < 0.04$ .

copper, whereas the spectrum for carbon remains regular. Fits of the  $pK_S^0$  mass spectrum for the  $hCu$  collisions under the selection  $x_F < 0.04$  are shown in Fig. 7a (bin 1.5 MeV) and Fig. 7b (bin 1 MeV). The fitting function is a Gaussian plus a third-order polynomial. The fitted mass of the peak is near 1539 MeV, and the width is consistent with being entirely due to instrumental resolution. (The Monte-Carlo prediction for a  $pK_S^0$  resonance of zero intrinsic width is  $\sigma_m^{MC} = 2.00 \pm 0.06$  MeV.) This allows to restrict the intrinsic width of the observed resonance to  $\Gamma < 3.0$  MeV at 90% CL. The statistical significance of the signal, estimated as  $S/\sqrt{B}$ , is near  $9\sigma$ .

In order to rule out a reflection from any  $K^+K_S^0$  resonance, we have assigned the kaon mass to proton candidates in the  $pK_S^0$  pairs with  $x_F < 0.04$  selected in  $hCu$  collisions. The resultant  $K^+K_S^0$  mass distribution proves to be regular. In order to verify that the peak is not an artifact of detector acceptance for copper targets, we have (i) reflected the

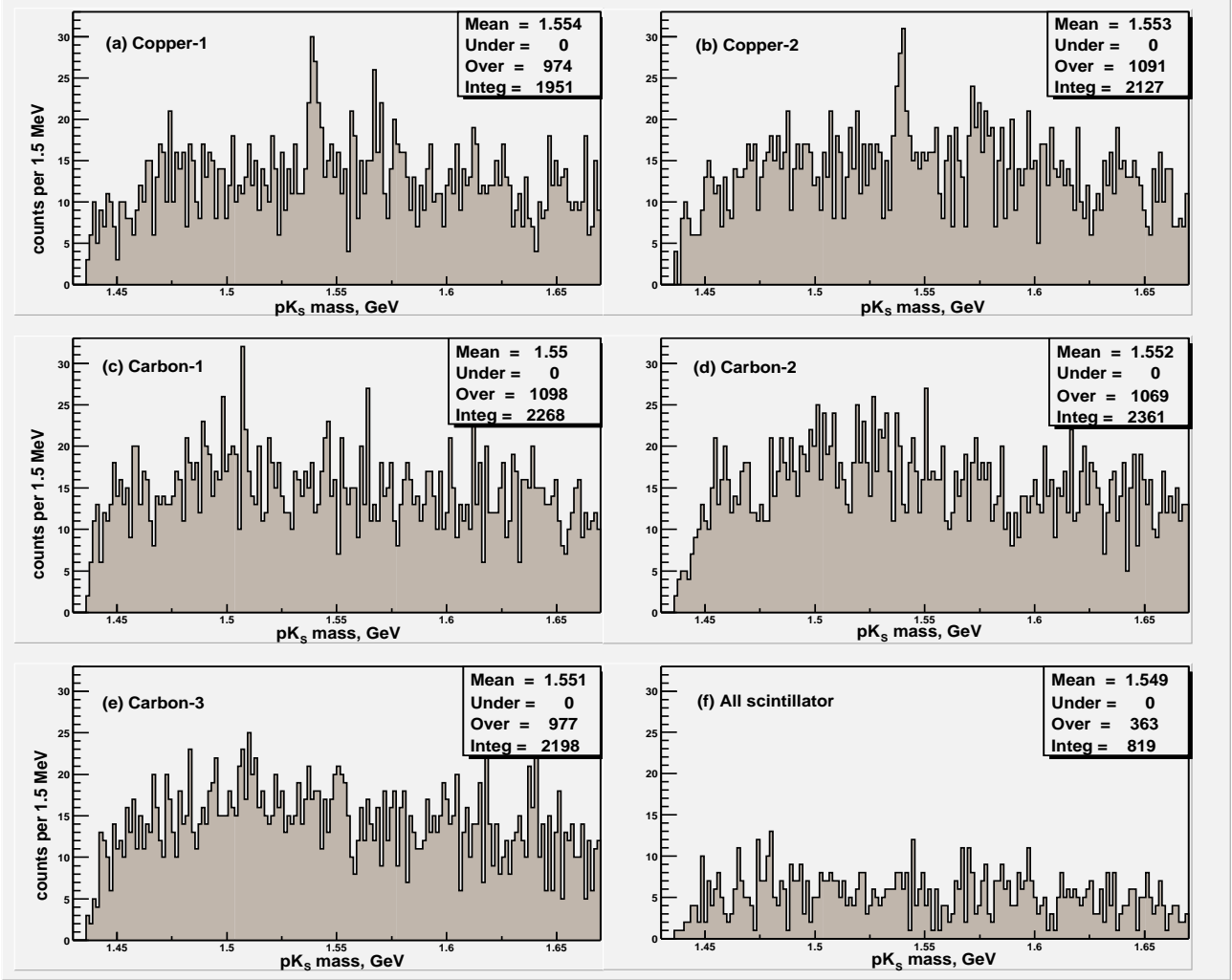


Figure 5: Breakdown of the  $pK_S^0$  mass spectrum for  $x_F < 0.04$  to five targets proper plus scintillator. The data for the three layers of scintillator have been combined.

transverse components of the  $K_S^0$  lab momentum,  $p_x \rightarrow -p_x$  and  $p_y \rightarrow -p_y$ , in selected  $pK_S^0$  pairs with  $x_F < 0.04$ , and (ii) assigned the proton mass to identified  $\pi^+$  mesons and then applied exactly the same selections as in Fig. 7 to the  $pK_S^0$  pairs formed by these “fake” protons. In either case, the resultant  $pK_S^0$  mass spectra prove to be featureless. A  $pK_S^0$  peak may conceivably arise from the decays  $\Lambda(1520) \rightarrow pK^-$  with a subsequent charge-exchange transition  $K^- \rightarrow K^0$ . However, the simulation suggests that such a reflection from  $\Lambda(1520)$  should occur at a lower mass (1515–1520 MeV) and have a width of several tens of MeV.

If the observed  $pK_S^0$  resonance is real and indeed has positive strangeness, a  $K^+$  emitted in association with  $\Theta^+$  always signals formation of an additional  $s\bar{s}$  pair. Therefore, dropping those events that feature identified  $K^+$  mesons among secondary particles should reduce the combinatorial background rather than the  $\Theta^+$  peak. Likewise, a  $pK_S^0$  resonance

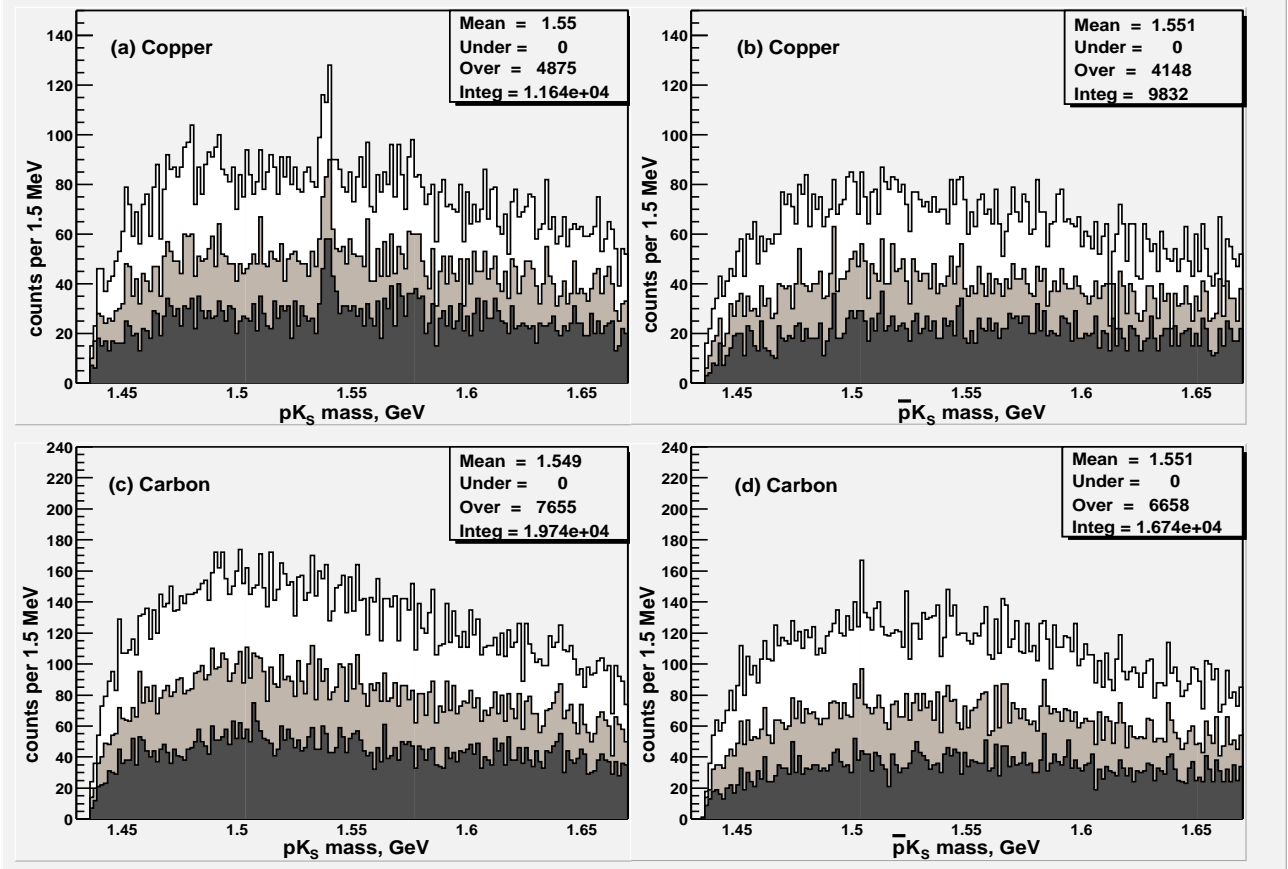


Figure 6: The  $pK_S^0$  effective mass separately plotted for collisions with copper and carbon under the selections  $x_F < 0.06$ ,  $0.05$ , and  $0.04$  (the open, shaded, and dark histograms, respectively).

of negative strangeness should be emphasized by dropping events with identified  $K^-$  mesons. We identify charged kaons as tracks with  $p < 200$  GeV, for which the kaon probability is the highest according to RICH information (PID = 4). Indeed, the signal in Fig. 7 is virtually unaffected by dropping events with identified  $K^+$  mesons, and depleted by dropping those with identified  $K^-$  mesons. This suggests that the observed  $pK_S^0$  resonance has positive rather than negative strangeness.

In order to have a closer look at the  $x_F$ -dependence of the peak, the  $pK_S^0$  mass spectra for successive bins of  $x_F$  are fitted upon fixing the Gaussian's position and width to  $m = 1539.5$  MeV and  $\sigma_m = 2$  MeV. The fitted signal as a function of  $x_F$  is shown in Fig. 8a for collisions with copper. Note that the  $x_F$  dependence is strongly distorted by detector acceptance, which steeply decreases towards negative values of  $x_F$  where the  $K_S^0$  mesons and protons are too soft to be detected and/or identified. We estimate the

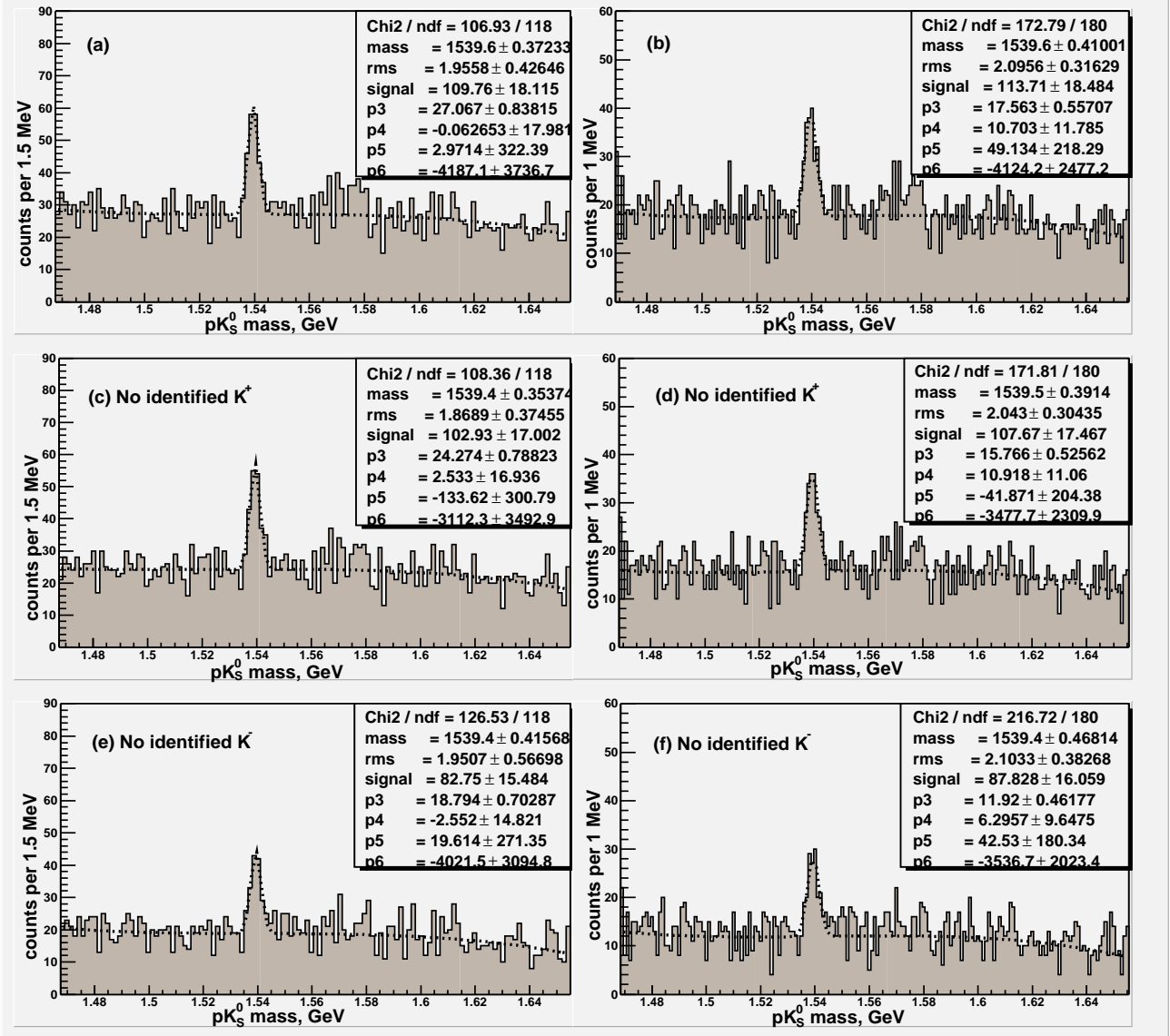


Figure 7: The  $pK_S^0$  mass spectrum for  $hCu$  collisions under the selection  $x_F < 0.04$  with mass bins of 1.5 MeV (a) and 1 MeV (b). The effect of rejecting events with identified  $K^+$  mesons is shown in (c) and (d), and of those with identified  $K^-$  mesons — in (e) and (f).

acceptance as a function of  $x_F$  through an EMBED-style simulation of  $\Theta^+$  production and decay, assuming isotropic angular distribution in the  $pK_S^0$  rest frame and  $\langle p_T \rangle = 1$  GeV. The acceptance-corrected signal as a function of  $x_F$  is shown in Fig. 8b. In collisions with copper, the acceptance-corrected number of events with  $\Theta^+ \rightarrow pK_S^0$ ,  $K_S^0 \rightarrow \pi^+\pi^-$  is estimated as  $(3.6 \pm 0.6) \times 10^4$  for  $0 < x_F < 0.06$ . The corresponding number for collisions with carbon is  $(0.3 \pm 0.7) \times 10^4$ . For the ratio between  $\Theta^+$  yields per collision in carbon and copper, we obtain an upper limit  $Y_\Theta^C/Y_\Theta^{Cu} < 0.24$  at 90% CL.

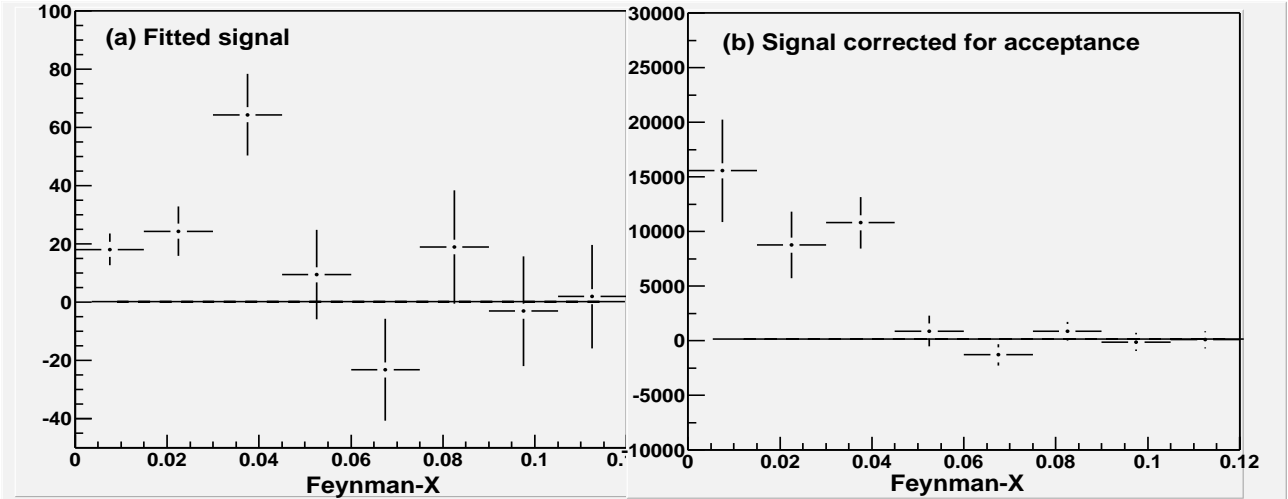


Figure 8: The fitted signal as a function of  $x_F$  for collisions with copper (a). The acceptance-corrected signal is shown in (b).

Assuming that the branching fraction for  $\Theta^+ \rightarrow pK^0$  is 50%, the total number of  $\Theta^+$  baryons produced with  $x_F > 0$  in collisions with copper is estimated as  $(2.1 \pm 0.4) \times 10^5$ . In the same experiment, the total cross sections of  $\Sigma^-$ -Cu and  $\pi^-$ -Cu collisions have been measured as  $1232 \pm 233$  and  $1032 \pm 179$  mb per nucleus, respectively [24]. Conservatively assuming that all detectable  $\Theta^+$  events were logged on tape and using  $7 \times 10^9$  inelastic collisions with copper for reference, we obtain  $\sigma(h\text{Cu} \rightarrow \Theta^+ X) = 37 \pm 10 \mu\text{b}$  for  $x_F > 0$ .

To conclude, a narrow enhancement near 1539 MeV is observed in the mass spectrum of the  $pK_S^0$  system formed in the region of target fragmentation ( $x_F < 0.04$ ) in hadron collisions with copper nuclei at 400–700 GeV. The statistical significance of the peak is near 9 standard deviations. Fitted width of the observed  $pK_S^0$  resonance is consistent with being entirely due to experimental resolution, and its intrinsic width is restricted to  $\Gamma < 3$  MeV at 90% CL in agreement with the direct measurement in [10]. The data favor positive rather than negative strangeness for the  $pK_S^0$  resonance observed in  $h\text{Cu}$  collisions. At the same time, the  $pK_S^0$  mass spectrum for collisions in carbon is featureless. The yield of  $\Theta^+$  baryons per  $h\text{C}$  collision is restricted to be  $< 24\%$  of the yield per  $h\text{Cu}$  collision.

## References

- [1] M. Gell-Mann, Phys. Lett. 8, 214 (1964);  
R.L. Jaffe, Phys. Rev. D15, 281 (1977);

- A.T.M. Aerts, P.J.G. Mulders, and J.J. de Swart, Phys. Rev. D17, 260 (1978);  
M. de Crombrugghe, H. Hogaasen, and P. Sorba, Nucl. Phys. B156, 347 (1979).
- [2] D. Diakonov, V. Petrov, and V. Polyakov, Z. Phys. A359, 305 (1997).
- [3] D. Diakonov and V. Petrov, Phys. Rev. D72, 074009 (2005);  
C. Lorce, Phys. Rev. D74, 054019 (2006);  
A.G. Oganesian, JETP Lett. 84, 409 (2006), arXiv:hep-ph/0605131;  
A.G. Oganesian, Int. J. Mod. Phys. A22, 2093 (2007), arXiv:hep-ph/0608031;  
Cedric Lorce, Phys. Rev. D74, 054019 (2006);  
Tim Ledwig, Hyun-Chul Kim, and Klaus Goeke, Phys. Rev. D78, 054005 (2008);  
Tim Ledwig, Hyun-Chul Kim, and Klaus Goeke, Nucl. Phys. A811, 353 (2008).
- [4] T. Nakano *et al.* (LEPS Coll.), Phys. Rev. Lett. 91, 012002 (2003).
- [5] V. V. Barmin *et al.* (DIANA Coll.), Yad. Fiz. 66, 1763 (2003) and Phys. At. Nucl. 66, 1715 (2003).
- [6] A.E. Asratyan, A.G. Dolgolenko, and M.A. Kubantsev, Yad. Fiz. 67, 704 (2004) and Phys. Atom. Nucl. 67, 682 (2004), arXiv:hep-ex/0309042.
- [7] T. Nakano *et al.* (LEPS Coll.), Phys. Rev. C79, 025210 (2009).
- [8] V.V. Barmin *et al.* (DIANA Coll.), Yad. Fiz. 70, 39 (2007) and Phys. At. Nucl. 70, 35 (2007).
- [9] V.V. Barmin *et al.* (DIANA Coll.), Yad. Fiz. 73, 1 (2010) and Phys. Atom. Nucl. 73, 1168 (2010).
- [10] V.V. Barmin *et al.* (DIANA Coll.), Phys. Rev. C89, 045204 (2014).
- [11] V.V. Barmin *et al.* (DIANA Coll.), arXiv:1507.06001 [hep-ex].
- [12] Volker D. Burkert, Int. J. Mod. Phys. A21, 1764 (2006), arXiv:hep-ph/0510309.
- [13] M.V. Danilov and R.V. Mizuk, Phys. Atom. Nucl. 71, 605 (2008), arXiv:0704.3531 [hep-ex].
- [14] C.H. Hicks, Eur. Phys. J. H37, 1 (2012).
- [15] R. De Vita *et al.* (CLAS Coll.), Phys. Rev. D74, 032001 (2006).

- [16] M.J. Amarian *et al.*, Phys. Rev. C85, 035209 (2012).
- [17] M. Moritsu *et al.* (E19 Coll.), Phys. Rev. C90, 035205 (2014).
- [18] Dmitri Diakonov, AIP Conf. Proc. 892, 258 (2007), arXiv:hep-ph/0610166.
- [19] Ya. Azimov, K. Goeke, and I. Strakovsky, Phys. Rev. D76, 074013 (2007), arXiv:0708.2675 [hep-ex].
- [20] J.S. Russ *et al.* (SELEX Coll.), in *Proceedings of the 29th International Conference on High Energy Physics*, 1998, World Scientific, Singapore, 1998, vol. 2, p. 1259, arXiv:hep-ex/9812031.
- [21] J. Engelfried *et al.* (SELEX Coll.), Nucl. Instrum. Meth. A431, 53 (1999).
- [22] V. Matveev, *Pass 3 user guide*, SELEX internal note, September 2004.
- [23] M.I. Adamovich *et al.* (WA89 Coll.), Phys. Rev. C72, 055201 (2005), arXiv:hep-ex/0510013.
- [24] A. Dersch *et al.* (SELEX Coll.), Nucl. Phys. B579, 277 (2000), arXiv:hep-ex/9910052.